Warsaw University of Technology

FACULTY OF
POWER AND AERONAUTICAL ENGINEERING

Institute of Aeronautics and applied Mechanics

Final Project

Mechanics and Machine Design
Modelling and Computer Simulations in Mechanics

Modelling and Simulation of resonance flapping wing resonance propulsion

Aurelio García Lloris

Krzysztof Sibilski

Warsaw, 2017

ABSTRACT

This Project describes an analysis and design of a MAV Micro Air Vehicle. The aim of the project is to find some structure that can allow the resonance of the flapping-wing movement.

The study is focus in the structure of the concepts where different spring materials are studied to know which one fits better with the flexible structure desired. The concepts studied are based in the insect thorax-wings system which is a tuned resonant system.

The first step is the selection of two prototypes. Secondly, we select one of them of which is done a study of the motion equation with different simulations to stand out the main differences between them.

The project is divided into five parts. The first one presents briefly the objective of the project. Then, insect flight is described. The next part describes flapping wing MAVs where our two concepts are presented. Section below contains simulations and calculations. Last part, comprises conclusions based on examined instances.

Contents

1 Introduction

1.1 MOTIVATION

Throughout history of evolution, the nature has optimized its resources in order to maximize the performance of existing biological structures on our planet. This fact has motivated the search of concepts based in animals. For example, Leonardo Da Vinci designed a flying machine from the study on the bird anatomy, the Ornithopter.

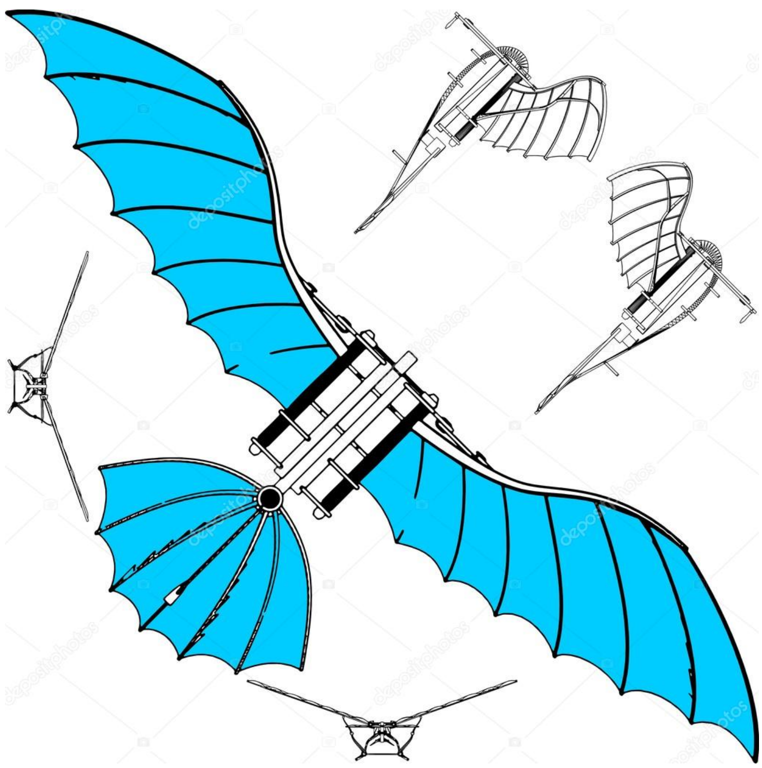

Figure 1: Leonardo Da Vinci's Ornithopter.

Last years, there have been great advances in different areas of science related to the design of artificial devices from the study and observation of organisms, systems and processes existing in nature. In many cases, a complete biological imitation of an insect, bird, or fish has been attempted, resulting in disappointing results. It is important to distinguish between what is meant by biological imitation, biomimetic, and inspiration in biology. The biomimetic or copy of an organism is very difficult to achieve with current technology, on the other hand, inspiration in biology, is a good starting point to take a first step towards the design and manufacture of robots that have a performance equal or greater than the biological entities existing in nature.

Nowadays, scientific community is focus in the development of MAVs, Micro Air Vehicle, inspired in the flight of the insects and little birds, like the hummingbird, that are able to perform complex movements.

1.2 MICRO AIR VEHICLE

The United States Defence Advanced Research Projects Agency, DARPA, has defined the MAV as any flying vehicle which is limited to 150 mm or smaller in any linear dimension.

We can differ between three types of MAVs, we find the fixed-wings MAVs, the rotary-wing aircraft and the flapping wing flyers.

The fixed-wing is the most efficient kind of MAV; it is able to run through longer distances but it has less mobility than the rest. The rotary-wing MAV, stands out because its ease of movements. The flapping wing flyers, are inspired by the nature. The advantages of this type of insect-inspired vehicles are greater versatility to perform complex manoeuvres, greater flight stability and lower energy consumption. It means longer flight times. Among the manoeuvres, it is able to perform low-speed flights, as well as take-offs and landings over short distances. Also, it can produce the same lift with smaller wing by the increasing of flapping frequency.

In this project, we are designing a flapping wing MAV. We try to fulfil the requirements from the Atalanta Project. Our MAV should be able to fly autonomously, hover and fly slowly, communicate with others and a base station, manage power, provide payload capacity and be adaptable for many situations.

1.3 BACKGROUND

The implementation of flapping flight at the smaller scales is much more difficult than fixed-wing and rotary-wing implementations. Nevertheless, it is interesting to strive for insect flapping-wing MAVs due to some reasons.

The first reason, it is the flying speed. Due to flapping wing system, we stay airborne in low velocities producing lift with the wings movement. Secondly, insects and birds combine control and propulsion in their flapping wing systems while rotary-wings and fixed-wings MAVs need additional actuators for control, additional rotors in rotary-wings and control surfaces in fixed-wings.

Because of their ability to hover, we can look birds, bats and insects to get some ideas. But the size range of flapping wing MAVs makes us pay close attention in insects. Firstly, we notice the system that drives the wings. In insects the whole thorax structure functions as a spring and combined with the wings essentially forms a tuned mass-spring-damper system. The wings in insects are predominantly passive structures. The absence of active elements in the wings make insects more suitable for inspiration of flapping-wing MAVs.

Along history, attempts have been made to imitate the insects flapping-wing flight. In spite of the advances in this kind of MAVs last decade, the biological entities stay ahead of manmade prototypes. The most common problems that we can find are size problems and autonomy of the flapping-wing MAV.

1.4 PROJECT STRUCTURE

The Project is divided in five main parts.

- The Introduction describes briefly general points that we are looking in the rest of the work.
- Secondly, we get information about the insects, its anatomy and its flight.
- The third part is a study of the MAVs, in particular the flapping wing MAVs. Based in the insects, we choose the prototypes that we will study.
- Consecutively we put the prototypes to some test to carry out an analysis.
- Finally, we get some conclusions about the study performed in the fourth part.

2 Insects

2.1 INSECTS ANATOMY

When you are designing and constructing a MAV, an important aspect is to understand how insects and small birds flap their wings to produce enough lift and thrust to fly and to drive around the air.

There are a lot of experimental works about the study of insect aerodynamics, which provide a good description of the non-conventional aerodynamic mechanisms used by these creatures to stay in flight. On the other hand, a precise quantitative description of such phenomena is difficult to achieve due to the errors in the techniques used to perform measurements of the magnitudes of interest.

When looking at insects as inspiration, two aspects are interesting. First, the insect thorax, it produces the power and drives the wings. Second, the wings which are an integral part of the flight mechanism.

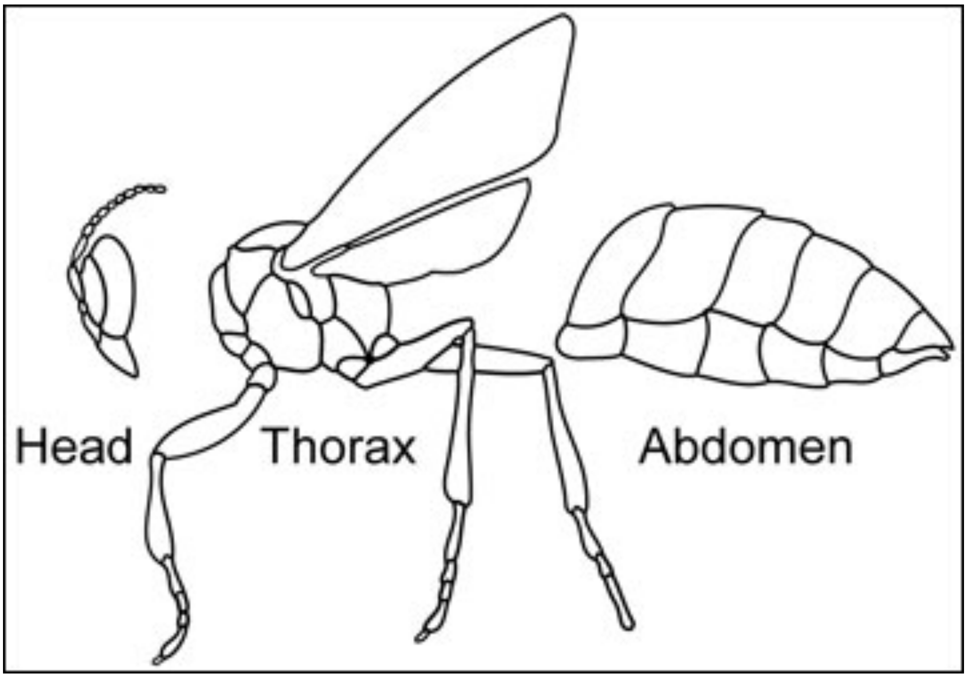

Figure 2: Body of insects.

The insect consists of three body parts, the head, thorax and abdomen. The head carries the brain and perceive vision, olfactory and hearing. The abdomen contains the reproductive organs, breathing apparatus and most of the digestive system. As we mentioned before, the thorax is one of the most interesting aspects in the flight of the insects because it produces the power and drives the wings. It has the wing actuation mechanism.

From an engineering viewpoint the wing-thorax structure is a compliant amplification mechanism. Two different thorax designs exist which differ in the way the wings are driven: direct and indirect.

In the direct-drive mechanism, the muscles drive the wings directly. The different wings, it is possible with this mechanism to find two or four wings, can have different flapping frequencies and amplitudes, allowing a very large range of force production and large aerial agility.

The indirect-drive mechanism produces higher wing-beat frequencies than direct-drive mechanism. The deformation of the thorax is governed by two muscle groups. The elastic properties of the thorax and muscles combined with the inertial properties of the wings and the thorax box form a tuned mass-spring-damper system.

For application in flapping-wing MAVs, the indirect-drive mechanism is most interesting because the resonant properties.

The wings are, as seen from an engineering viewpoint, a structure which consists of load bearing members, longitudinal veins, crossbeams, cross-veins, and spanning between the veins and cross-veins is a sheet, membrane.

Being passive structures, the wings are driven at the base where they connect to the thorax through the wing joint. The wings constitute the major part of effective inertia of the moving thorax-wing system.

The resonant properties help to reduce the inertial cost of the wing movement. As we mentioned, the insect-thorax wing system can then be seen as a tuned mass-spring-damper system. The mass is dominated by the inertia of the wings. The spring function is a combination of the elastic thorax shell and the muscle properties. The aerodynamic loading on the wings can be seen as the damping force.

2.2 WING MOVEMENT

The insects wing movement can be separated in two parts: a rigid body motion and an elastic deformation. The rigid body motion consists of three rotations facilitated by the wing-root joint. The elastic deformation consists mostly of torsional deformation and bending. The magnitude of the elastic deformation is small compared to the rigid body movement.

The three rotations that compound the rigid body motions are the main sweeping angle, the wing pitching motion and the out of plane motion.

The main flapping or sweeping angle, which is the most characteristic motion of the wing, makes the wing trace a plane which is approximately horizontal for most hovering insects. The main flapping is the result of the resonant motion and as such is described by a harmonic motion.

The second motion, the wing rotation or wing pitching, is defined as the rotation of the wing about its radial axis. This motion, together with direction induced flow, defines the angle of attack of the wing. The wing pitching is generally a motion close a pure sinus. The frequency of the pitching motion is always the same as the main flapping motion whit a phase shift between both. The origin of wing pitching has been the subject of argument among biologists. Analysis of the insect thorax suggest that the control muscles are too small to generate the required power for wing pitching. However, pitching could be the result of a smart wing-root hinge configuration. The second option is passive pitching controlled by inertial and aerodynamics loads. The general consensus among biologists and engineers is that during steady-state flying or hovering wing pitching is passive. However, when the insects perform extreme manoeuvres indications are that the reconfiguration of the wing joint is such that wing pitching is at least partially actively controlled.

The last motion is the out of plane motion or heaving motion with describes the deviations from the stroke plane.

A typical wing stroke cycle van be roughly divided in four phases. The first are the up and downstroke. In these phases the wing moves with respect to the body with approximately constant wing rotation. The remaining two phases are the two stroke reversals, called supination after the down stroke and pronation after the upstroke.

For the majority of applications, the rigid body description suffices. However, the elastic deformation carried out by bending and torsion play a role in the insect wing kinematic.

The application of loads on the wings, both inertial and aerodynamic, results in wing deformation during the flapping motion.

While bending is present in insect-wings, the aspect of torsion is more important. Torsion and more specifically the timing of torsion and deformation during the wing stroke can directly influence the timing of torsion deformation during the wing stroke can directly influence the local wing pitching angle and, consequently, the local angle of attack.

When we talk about the elastic deformation of wings it is noted that the size is an important fact inasmuch as in the small insects the effects of bending and torsion are more reduced than in larger insects.

2.3 AERODYNAMICS

Flapping flight by insects is characterized by unsteady incompressible flow at intermediate Reynolds number. For large insects the Reynolds lies between 5000 and 10000. The smallest flying insects have Reynolds numbers which can go as low as 10. The range is large due to the wide variation in the body mass of the flying insects.

The production of lift and thrust follows from the complex interaction between the compliant wings, wing kinematics and the aerodynamics. Aerodynamic theory is well developed for larger scales and can be applied at insect scale with the incorporation of effects that are present at these smaller scales and, consequently, lower velocities. The flapping wing induces unsteady flow with a cyclic nature.

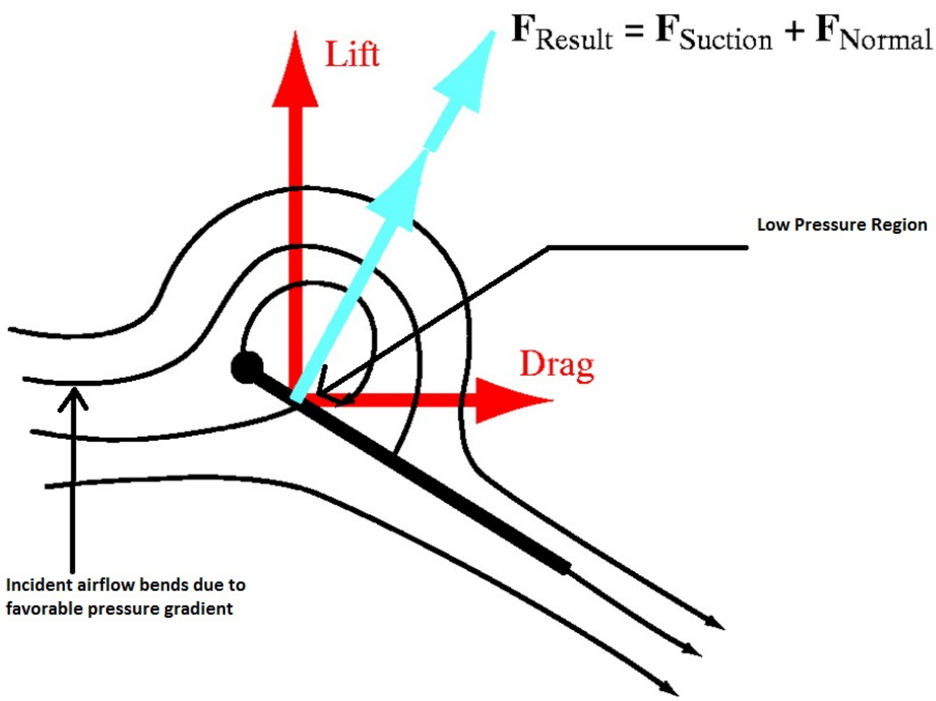

Figure 3: Insect Aerodynamic.

The production of lift and drag in insects is based on three mechanisms, the leading edge vortex, the rotational circulation and the wake capture.

The leading is the most important aerodynamic effect in insect flight. Due to this LEV the flapping insect wing produces far more lift than can be explained using normal airfoil theory. Experiments show that when a wing moves through the air, a large vortex starts at the leading edge of the wing and forms on the top of the wing. The rotation in this vortex is very high. The associated high velocity creates a patch of low pressure on the wing surface facilitating lift production. This vortex grows in size during wing flap and after some chord lengths releases from the wing and removing the low pressure field and thus lift.

The rotational circulation effect is only present during phases where the rotational or pitching velocities are large, the stroke reversal. By varying the wing rotation timing and rotation speed, causing advancements or delays in the wing kinematic pattern, the wing forces can be varied. The force will increase when the rotation is advanced and decreased when the rotation is delayed. The rotational speed of the wing contributed to extra lift.

The wake capture is the effect where flapping wings interact with the vortex that was shed at the end of the previous stroke. This creates large load peaks at the beginning of the new stroke. This increase in lift is caused by the increase in fluid flow by the capture of the previous vortex. The wake capture effect is most pronounced during stroke reversal and not during the period of relatively low pitching velocities during mid stroke.

Two other effects are present in insects but are not directly responsible for lift production. The first is the effect of added mass or virtual mass. The virtual mass can be seen as a region of influence where the air around the wing moves with the wing and contributes to the effective inertia of the wing. The other effect is known as clap and flight. The effect consists of expanding the wing sweeping angle so far the wings touch at the end of the upstroke above the body of the insect. When the downstroke starts the wings are rolled open in order to jump start the LEV. Since the formation of the LEV is independent of wing size, jump starting might be beneficial for very small insects which have a very small wing stroke in absolute sense.

2.4 KEY POINTS

As we mentioned, direct copy of insects is not possible with nowadays science. However, to produce a great flapping-wing MAV we need to look in detail the insects because they are such successful flyers.

The most important points are the body or the thorax of the flapping wing MAV, the wing transmission system and the wings.

The goal about the thorax is the application of the resonant principles which are present in the insects. Therewith, we reduce the energy impact of wing movement and we obtain a large wing sweeping stroke. Besides, we need to take care because same drawbacks are introduced.

The wing sweeping frequency becomes bounded by high sensitive to changes in drive frequency. This mechanical equivalent could be an elastic element to store the kinetic energy. Besides that, we need a mechanical equivalent for the thorax structure in insects that participates in the resonant thorax-wing system, it should strive for a very high degree of integration.

The thorax is driving the wings so the thorax deformation has to be transformed and amplified into a large sweeping motion in the wing base. In insects this property is integrated into the thorax-wing-root combination. The thorax and wing root together form a fully compliant system capable of generating complex kinematics.

Wing pitching also finds its origin in the wing root. MAVs thorax would be amendable to accomplish the same features.

The wing is the place where lift is produced. It will pose a significant challenge to design a mechanical equivalent if the insect wing. As we see before, the wing pitching may be of passive origin. In the ideal case, the timing and amplitude of wing pitching will have to be obtained by a combination of a highly compliant wing root with a wing which is able to support a beneficial torsional wave to augment lift production. The system has to be designed in a highly integrated fashion.

3 Flapping Wing MAVs

3.1 BACKGROUND

The design of flapping wing MAVs is still a very active area of research. While the model plane world has known small rubber band powered ornithopters since the 1870s, the first electric powered flapping wing MAV, named the MicroBat, only flew in 1998. The design of flapping wing MAVs until now mainly progressed by means of trial-and-error. Automatic optimization is still very unreliable due to a lack of accurate theoretical models. Especially the design decisions concerning the shape, tension, and materials of the wings cannot be made purely on the basis of simulation due to a lack in knowledge on the aerodynamics around flexible airfoil.

Historically, flapping-wing MAVs have been based on bird-like flight focussing on forward flight. Nowadays, these designs are inspired by small birds and insects because hovering and slow moving is interesting for possible indoor usage.

To analyse the past designs is a good option to start. We can see what is being done in the field and we can extract some ideas and good practice similar to the analysis of insects.

An aircraft design is highly dependent on the intended use of the platform. The driving force in the design can be to optimize for maximum endurance on one hand, or on the contrary to optimize for minimum size. Typically, the goal also includes other aspects such as stability or payload capability. Different combinations of goals can lead to very different designs. Common to almost all of these goals is that they are harder to attain at smaller scales. There are coarsely two approaches to finally arrive at fully functioning fly-sized flapping wing MAVs: bottom-up and top-down.

The bottom-up approach focuses on constructing and testing the tiny parts necessary for directly constructing a fly-sized robot. Research studies adopting this approach often tackle extremely difficult sub-tasks such as the construction of the insect thorax, or the generation of sufficient thrust.

The top-down approach starts with relatively larger scale but fully functioning flapping wing MAVs. The idea behind the approach is that studying such MAVs can lead to insights for the construction of a following, smaller or smarter version. One advantage of this approach is that it allows interplay between theory and practice. For aerodynamics research, having a flying system ensures that the research is directed to aspects that also have a practical relevance. For artificial intelligence research, having a physical and fully functioning MAV is of great value: real-world tests force the experimenters to take into account all aspects of the robotic system. In addition, they reveal physical properties of the system that can be exploited by the algorithms.

The bottom-up and top-down approach have complementary advantages and risks. For example, a risk of the top-down approach is that the research will focus too much on incremental modifications of the MAV, ignoring possible disruptive improvements. On the other hand, a risk of the bottom-up approach is that research may focus too much on detailed aspects that might turn out irrelevant for a fully flying system. The bottom-up approach can lead to fundamental new understanding and techniques, while the practical 'surprises' of the top-down approach give insight into pressing problems of lacking scientific knowledge or technology. We believe that progress in flapping wing research requires both approaches to exist.

3.2 WINGS

Various methods exist to manufacture wings for flapping-wing MAVs. The most common method of constructing is the method of spanning a membrane by stiff rod type structures. Other methods for constructing wings usually rely on using a membrane and stiffening structure which represents a vein like structure.

Passive rotation characteristics have a strong dependence on the detailed shape and mass distribution of a wing. Natural and artificial wings display great variation in size, platform, material composition, and vein structure. Development of a concise wing parameterization is required.

Among the existing and functional MAVs, three types of wing configurations, monoplanes, biplanes and folding wings are distinguished. The monoplanes consist of a pair of wings that oscillate in phase. The advantage they present is a lower final weight and as a disadvantage it is more instable and it has more amplitude of rolling.

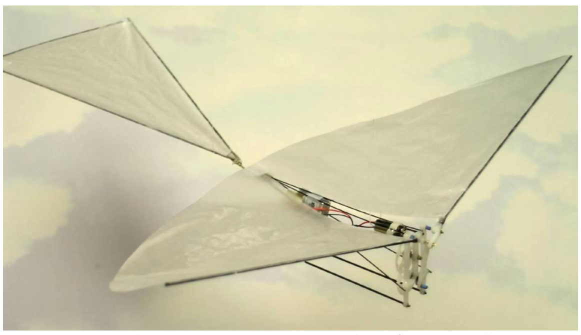

Figure 4: The MicroBat, example of monoplane.

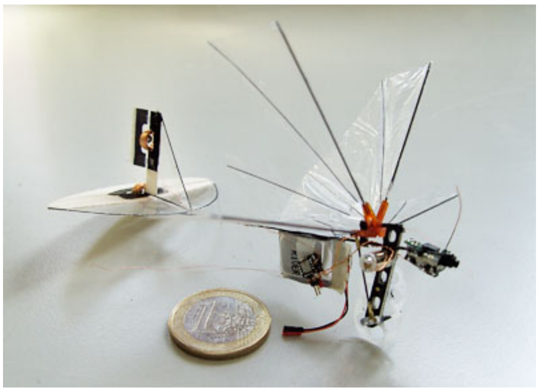

Figure 5: The Delfly, example of biplane.

Biplanes consist of two pairs of wings that move in phase. These wings can be one behind the other or one over the other. The advantage of this configuration is a lower rolling range and greater stability. The disadvantage is an increase in the weight of the vehicle.

Finally, the folding wings are folded to simulate the flight of birds. The wings extend when the movement is downward and fold to the body as they rise, thus reducing the area which minimizes the negative lifting effect. The disadvantage of this configuration is the excessive weight of actuators making it difficult to implement in MAV.

The wing design is very important for the aerodynamic performance, and hence the lift that can be generated by the flapping wing MAV. It involves a choice of the materials for the structuring elements and wing membrane, and the way to combine these to form the wing’s shape and structure. A traditional choice for the wing materials consists of PET-foil and carbon fibber reinforced polymer (CFRP) rods. These materials have proven their worth, are widely available, and do not require specific infrastructure for construction. The downside is that they typically require some manual work, which can limit repeatability. Moreover, the design options with these materials are relatively limited. Most designs with PET-foil and rods are limited to geometric shapes with a stiff leading edge and a few stiffeners added to the wing. In order to allow for more intricate, and yet repeatable designs, other materials and fabrication methods have been investigated.

The currently available wing technologies are suitable for the current insect sized flapping-wings MAVs, however, improvements can be expected.

3.3 ACTUATORS

The function of the actuators is to activate some process in order to achieve the control of the process. There are various types of actuators, mechanical, hydraulic…. The most common in the design of MAV are servos motors and magnetic actuators due to low weight. They are able to deliver a smooth and proportional control to the signal.

In order to choose one actuator technology or another, the actuators have to be checked if they live up to the boundary conditions which are imposed by a flapping-wing MAV. The design of the flapping-wing MAV is highly influenced by the choice of the actuator.

Magnetic actuators are pulse width modulation (PWM) driven with a duty cycle proportional to the transmitter control stick, which results in a proportional current. This current produces a moment in the magnet which again translates to a proportional force that goes to the control surface. However, the force is small and with the air pressure on the control surfaces being proportional to the air velocity squared, the control throw gets much lower at higher airspeed. This can cause inability to pull up from fast descending flight.

An alternative consists of conventional servos that use a small electric motor, gearing and a potentiometer or magnetic-hall sensor for position feedback. This type of actuator has more force and a higher accuracy compared to the magnetic actuator.

Due to the trend of miniaturization and the availability of manufacturing techniques, piezoelectric actuators have been used for micro devices. Application in flapping-wing MAVs is complex due to medium to high voltages needed for actuation, and the corresponding need for high voltage electronics. Piezoelectric actuators allow a high velocity movement of the wings with a small amplitude.

Not all mentioned actuator technologies are equally feasible. Implementation effort for the application of a specific actuator technology depends on the size of the intended flapping-wing MAV.

3.4 DESIGN

As we have seen, the source of inspiration is the insects. However, a direct translation from the insect thorax to engineering equivalent is not possible or desired, because technical solutions follow different guidelines and use different materials rather than biological structures.

The requirements for the current developments of the wing actuation mechanism for the flapping-wing MAV are geared towards the implementation of resonant principles while maintaining a very simple design.

The application of resonance in flapping-wing MAV is based in the storage of potential energy in a deformable structure. This is focus in four properties: The material used, the volume of the material, the deformation mode and amount of deformation.

The deformation mode used to store potential energy has large influence of the thorax structure. The deformation modes which can be used are compression, bending, torsion and shear of a material which can store energy efficiently. Combinations of deformation modes are possible.

In order to put boundaries on the designs, four main aspects influence the design and provide design directions.

- Simplicity: Based on the fact that simpler designs seem to be more successful. Low complexity designs are usually of low mass and therefore provide better chances of lift-off.
- Resonance: The design has to fully exploit resonance for maximum reduction of the power expenditure in accelerating and decelerating the wings.
- Passive wing pitching: This is a trade-off between aerodynamic efficiency and a low mass structure. Although actively pitched

wings are able to produce lift, the increase in mechanism complexity leads to an overall increase in mass.

3.5 CONCEPTS

Following the main concepts that we have seen along the project, we have the design of two concepts. These two concepts, are two winged design.

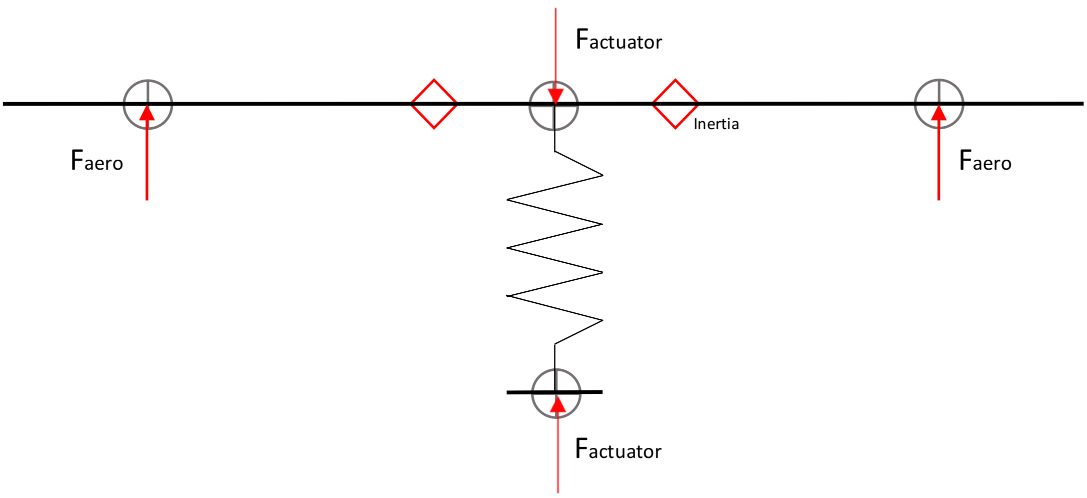

Figure 6: Concept 1

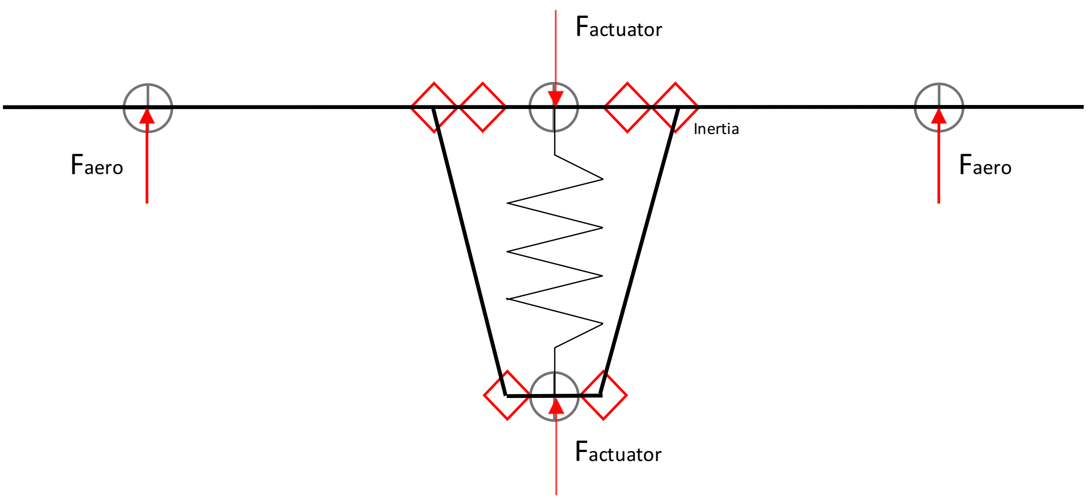

Figure 7: Concept 2

4 Analysis

4.1 MATHEMATICAL MODEL

The analysis will be done only for the concept 1 due to the complexity of the study for the second concept.

In this model study, we assume that the body weight is higher than the wing weight. The system is reviewed as being single degree of freedom represented by the wing sweeping angle ϕ.

The one-dimensional equation of motion is:

$$I\ddot{\phi} + k\phi = M_{act}(\dot{\phi}) - M_d(\dot{\phi})$$

Where:

- Inertia I represents the equivalent inertia of the system including both wings.
- K represents the spring constant.
- The torque of the aerodynamic forces are represented by M_d.
- The actuation M_{act} is applied as a torque at the wing root.

We suppose a harmonic forced motion based on simple harmonic wing sweeping motion so:

$$\phi = A\sin(wt)$$

$$\dot{\phi} = A\cos(wt) * w$$

$$\ddot{\phi} = -A\sin(wt) * w^2$$

Maximum amplitude A is restricted by the wing setup of the flapping-wing MAV.

The inertia I of a bar, wings, is:

$$I = m_w * L^2$$

- The mass of the wing is represented by m_w.
- L represents the length between the inertia centre and attachment point of the aerodynamics forces.

Using simplifications, we have:

$$M_{act}(\dot{\phi}) = I\ddot{\phi} + k\phi + M_d(\dot{\phi})$$

$$M_{act}(\dot{\phi}) = m_w * L^2 * (-A\sin(wt) * w^2) + k * A\cos(wt) * w \ + M_d(\dot{\phi})$$

$$M_{act}(\dot{\phi}) = m_w * L^2 * (-A\sin(wt) * w^2) + k * A\sin(wt) + M_d(\dot{\phi})$$

$$M_{act}(\dot{\phi}) = (k - m_w * L^2 w^2) * A\sin(wt) + M_d(\dot{\phi})$$

K can be replaced by natural frequency equation to highlight the importance of the resonance.

$$k = {w_0}^2 * m_w * L^2$$

$$M_{act}(\dot{\phi}) = m_w * L^2({w_0}^2 - \ w^2) * A\sin(wt) + M_d(\dot{\phi})$$

First part of equation, $m_w * L^2({w_0}^2 - \ w^2) * A\sin(wt)$, represent the overcome wing inertia.

The aerodynamic forces $M_d(\dot{\phi})$ can be approximated by:

$$M_d = \ C_{d,c} * L^3 * \dot{\phi}^2 * \frac{\dot{\phi}}{\sqrt{\dot{\phi}^2}}$$

After simplifications, we obtain the overcome drag:

$$M_d = \ C_{d,c} * L^3 * A^2 * w^2 * \left(\frac{1}{2} + \frac{1}{2} * \cos(2 * wt)\right)$$

- $C_{d,c}$ is defined as $\frac{1}{2}\ C_D * S * \rho$

$$M_{act}(\dot{\phi}) = m_w * L^2({w_0}^2 - w^2) * A\sin(wt) + C_{d,c} * L^3 * A^2 * w^2 * \left(\frac{1}{2} + \frac{1}{2} * \cos(2 * wt)\right)$$

We need to add the lift force to the model to keep the system hovering. The minimum lift to sustain the system hovering is given by:

$$F_l = (m_w + m_b) * g$$

Final expression of the torque at the wing root is:

$$M_{act}(\dot{\phi}) = m_w * L^2({w_0}^2 - w^2) * A\sin(wt) + 2 * \frac{C_{d,c}}{C_{l,c}} * L * (m_w + m_b) * g * \left(\frac{1}{2} + \frac{1}{2} * \cos(2 * wt)\right)$$

4.2 NUMERICAL DATA

We identify the known variables and we think about consistent measures.

The first step is the sizing of the concept. We consider the values applied by Bolsman in his PhD and the DelFly project. Our longitudes data will be:

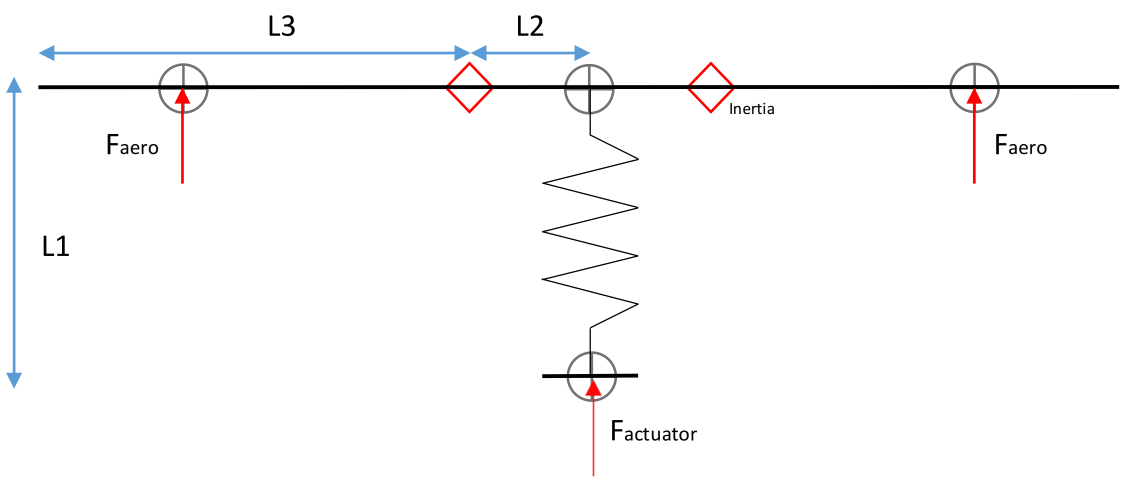

Figure 8: Concept 1 longitudes.

First sized concept	
L1	40 mm
L2	10 mm
L3	40 mm

Table 1: Concept 1 first sizing.

We will experiment with two different sized concepts. The other sizes are:

Second sized concept	
L1	50 mm
L2	15 mm
L3	60 mm

Table 2: Concept 1 second sizing.

When we have sized the concept, we estimate the mass of the system.

The overall mass of the system is the sum of mass of the wing and mass of the body.

Looking the numerical of Bolsman we assume a total mass of the second sized of 10'5 grams.

The wings materials assumed is the PET. This material has a density of ρ=1'34 $\frac{g}{cm^3}$. The width and the thickness of the wings are based on Bolsman numerical data.

With this data we can calculate the volume of the wings and we have the density so we can calculate the mass of the wings.

$$Volume = Thickness * Width * Lenght$$

$$m_w = Volume * \rho$$

Thickness	12 mm
Width	0’1 mm
$Length_1$	40 mm
$Length_2$	60 mm
$Volume_1$	0’048 cm^3
$Volume_2$	0’072 cm^3
Mw_1	0’064 g
Mw_1	0’096 g

Table 3: Wings Mass.

About the relationship between lift and drag, we assume by Ellington that the typical ratio between them is $0'1 \leq \frac{C_{d,c}}{C_{l,c}} \leq 0'25$.

During the process, we had serious problems to get the estimation of the stiffness of the spring, K.

At first, we choose two typical materials, spring steel AISI 302 and the Beryllium Cooper, for the springs and we find both values of the Young is Modulus.

Material	E
Beryllium Cooper	124’105 GPa
Stainless Steel AISI 302	180 GPa

Table 4: Young is Modulus

To get the spring is stiffness, we will use this equation:

$$K = \frac{Area}{Length} \frac{N}{m}$$

Due to that, we need to differentiate between the two different concept sizing. After an exhaustive search, we do not find information about the sizing of the spring, so we assume it.

Concept 1 First sizing	
Spring Length	4 cm
Spring Area	8 cm^2
Beryllium Cooper K	2’48*$10^9 \frac{N}{m}$
Stainless Steel AISI 302 K	3’6*$10^9 \frac{N}{m}$

Table 5: First sizing stiffness

Concept 1 Second sizing	
Spring Length	5 cm
Spring Area	15 cm^2
Beryllium Cooper K	3’72*10^9 $\frac{N}{m}$
Stainless Steel AISI 302 K	5’4*10^9 $\frac{N}{m}$

Table 6: Second sizing stiffness

After our calculations, we compare the results with the spring properties used by Bolsman and we notify that our results are not coherent. As we have not many information about the springs, we will use the stiffness used by Bolsman.

K_1	381’1 $\frac{N}{m}$
K_2	403’4 $\frac{N}{m}$

Table 7: Stiffness final values

4.3 TRANSMISSION RATIO

First simulation in the project is the analysis of transmission mechanism. The equation is:

$$T = \frac{\phi}{u}$$

ϕ is the output, it is the angle of deflection of the wing. u, the input, is obtained from the deflection of the ring. ϕ will be expressed in rad, u in meters.

In this section, we plot the relation for a deflection of 90º and 120º and an input of 20 mm and 30 mm. We assume the total deflection of the spring of 20 and 30 mm according to past studies about the flight of the insects.

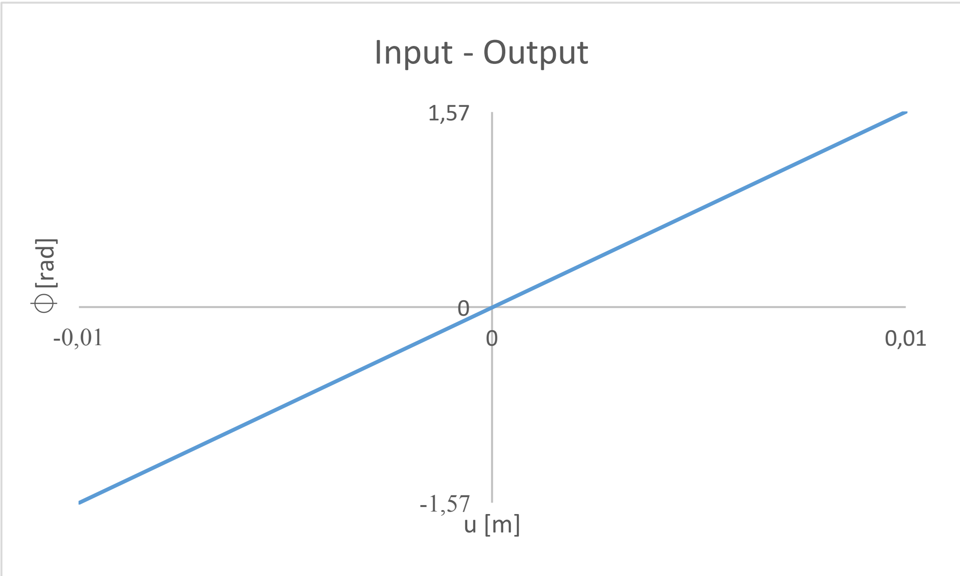

Figure 9: Relationship 20 mm – 90º

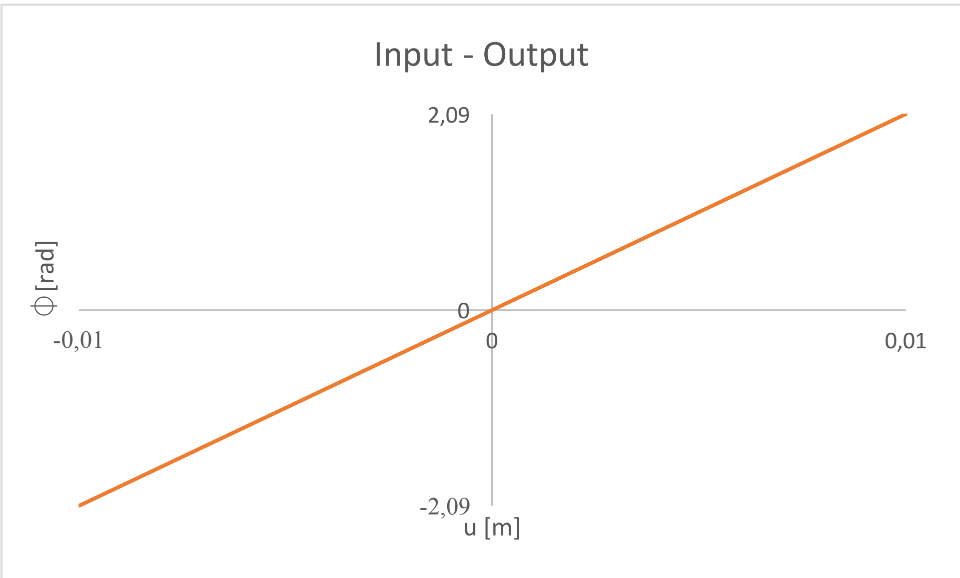

Figure 10: Relationship 20 mm – 120º

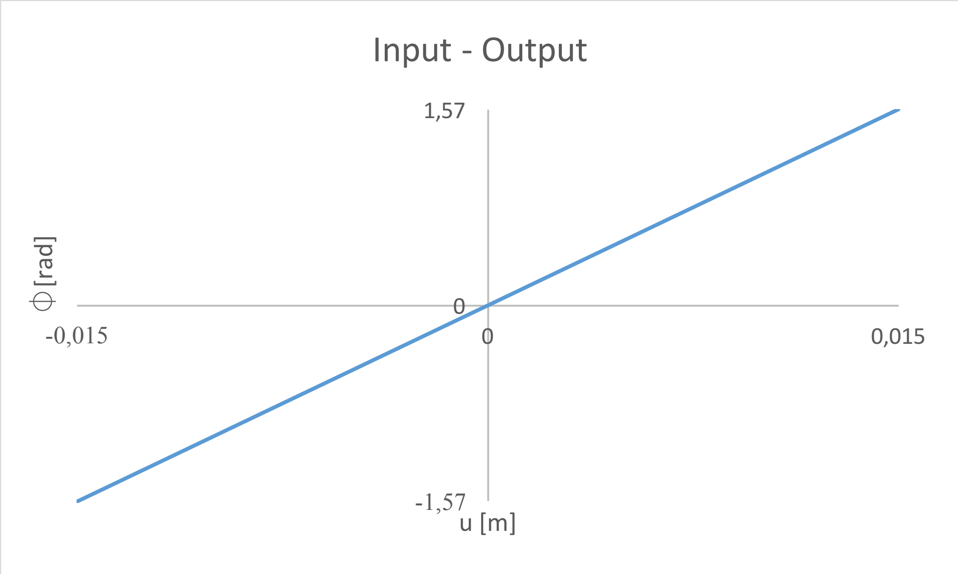

Figure 11: Relationship 30 mm – 90º

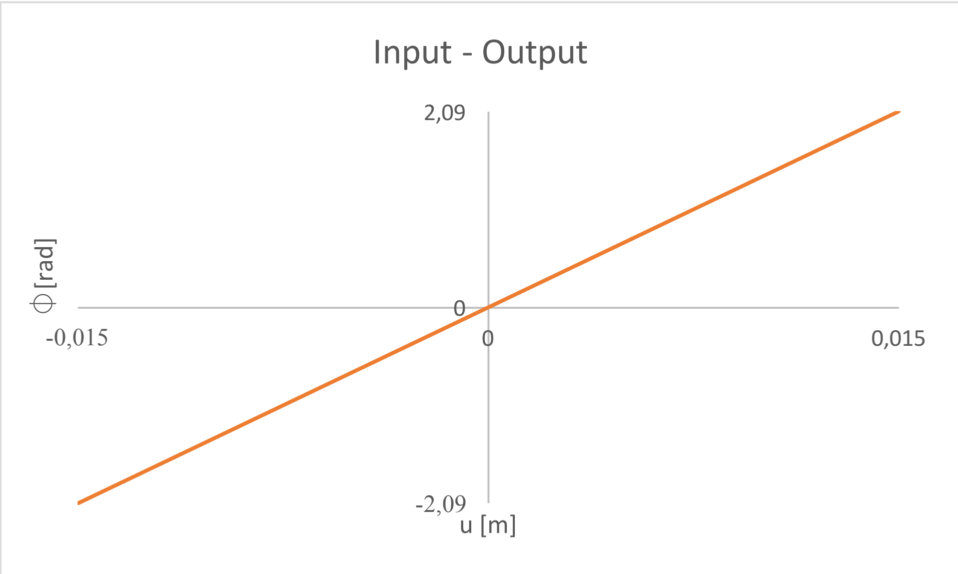

Figure 12: Relationship 30 mm – 120º

In the figures 9, 10, 11 and 12, we can see the linear approximation of the input-output relationship.

Below, we will study about the nonlinear movement because in the real case it becomes nonlinear in the degrees of deflection.

4.4 RESPONSE ANALYSIS

As we have commented along the project, our system has one degree of liberty and it is not dumped. We can represent our system as:

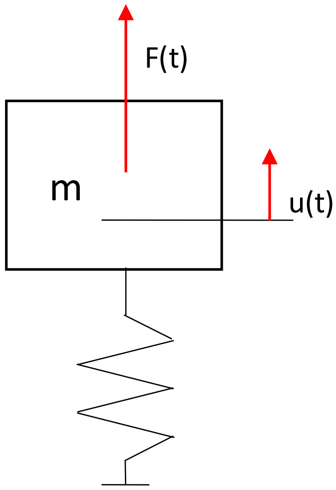

Figure 13: Representation of a system of one degree of liberty without dumper.

The movement equation of this system is:

$$m * \ddot{u}(t) + \ k * u(t) = f$$

We know that our system response is a harmonic simple response:

$$u(t) = A * \sin(w * t)$$

So the derivate transactions are:

$$u(t) = A * \sin(w * t)$$

$$\dot{u}(t) = A * \cos(w * t) * w$$

$$\ddot{u}(t) = -A * \sin(w * t) * w^2 = -w^2 * u(t)$$

As an external force we consider the aerodynamics force of our mathematical developed at point 4.1.

$$f = 2 * \frac{C_{d,c}}{C_{l,c}} * L * (m_w + m_b) * g * \left(\frac{1}{2} + \frac{1}{2} * \cos(2 * wt)\right)$$

The next step, is the calculation of the amplitude "A" of the harmonic simple response. For this measurement, we consider the time "t" equal to zero and with the help of the software Wolfram Alpha Mathematica we solve the equation to get the amplitude “A”.

$$A = \frac{2 * \frac{C_{d,c}}{C_{l,c}} * L * m_{total} * g}{k - m_{total} * w^2}$$

With the system developed, we can programme a code to do some interesting simulations about our concepts. For this simulations we use as we commented before Matlab software.

The first comparison is between the application of the natural frequency and other frequency. The rest of the values will be common for both simulations and we can look them in the following table:

m_{total}	10’5 g
k	381’1 $\frac{N}{m}$
$\frac{C_{d,c}}{C_{l,c}}$	0’1
L	0’1 m
g	9’8 $\frac{m}{s^2}$

Table 8: Common values for frequency representations.

The natural frequency is:

$$w_n = \sqrt{\frac{k}{m}}$$

$$w_n = 190'51 \frac{rad}{s}$$

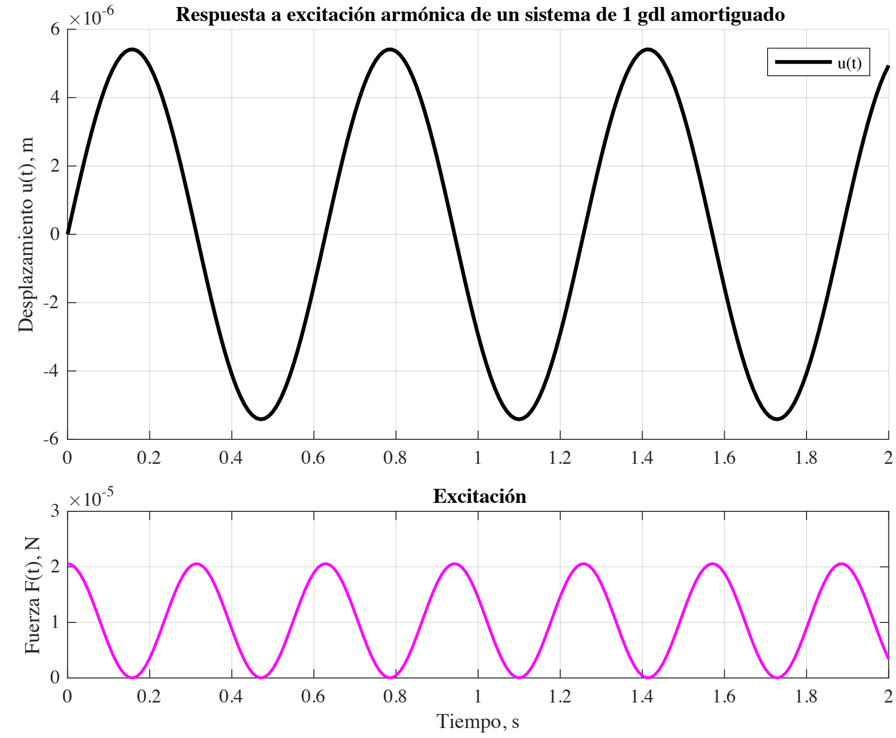

Figure 14: w=10 rad/s

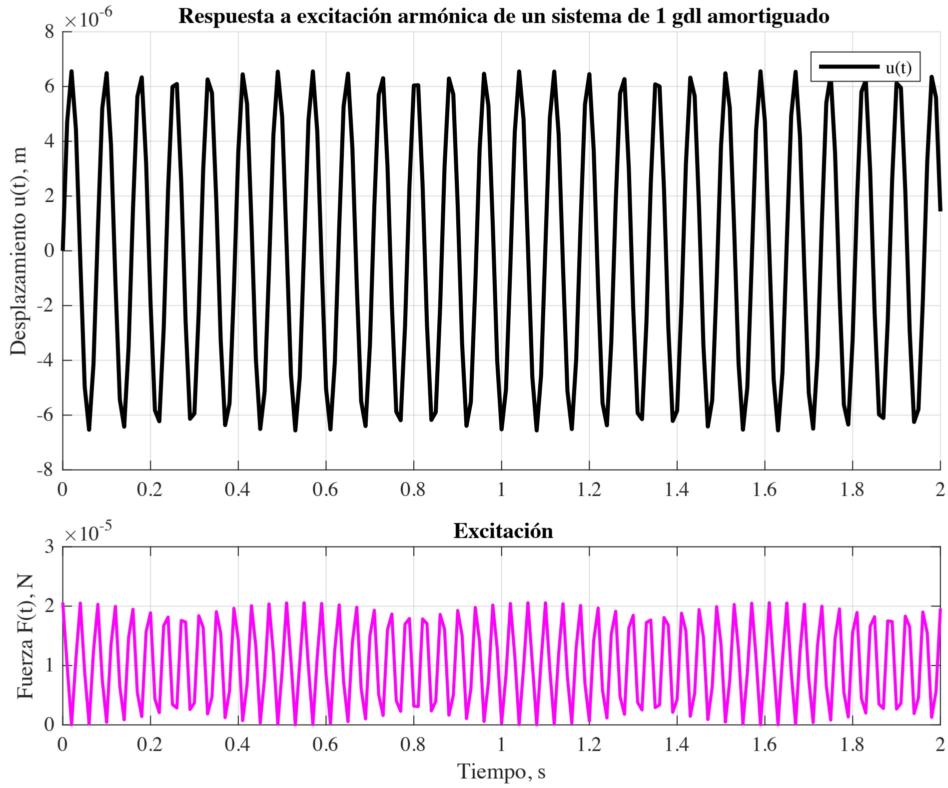

Figure 15: w=80 rad/s

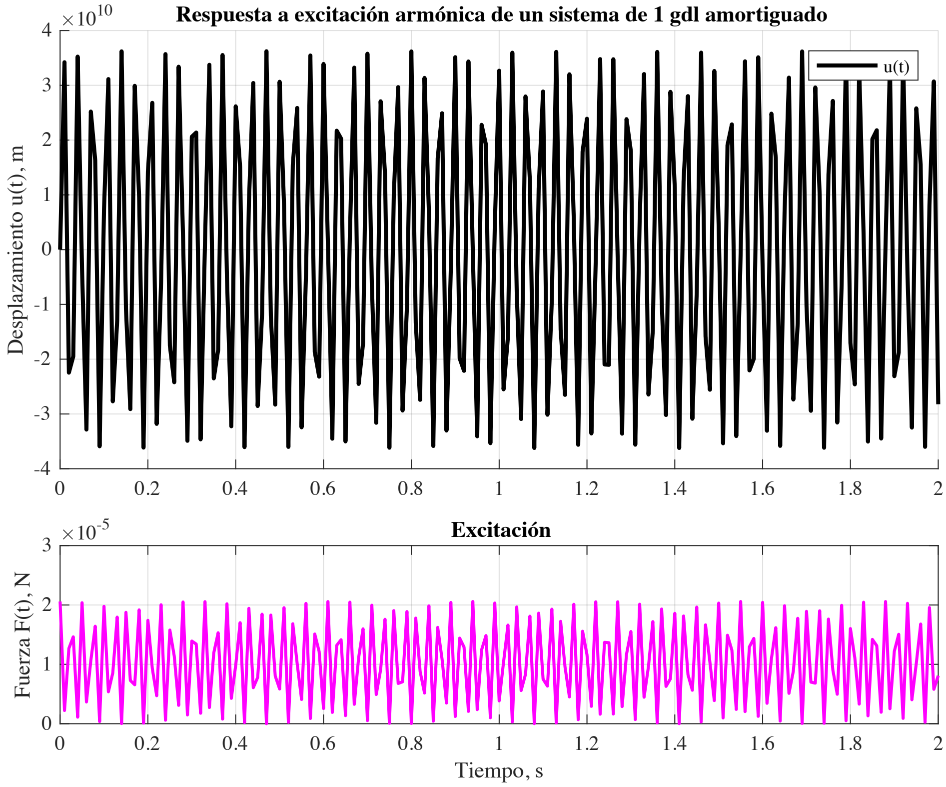

Figure 16: w=natural frequency.

Looking the different simulations, we can verify the sinusoidal response.

Inasmuch as we approach to the natural frequency, the displacement become higher.

As we can see, when the system is excited at the natural frequency, figure 16, we obtain the phenomenon of resonance. This is that we are looking for because we are trying to imitate the fly of the insect and as we saw, they use this phenomenon to move their wings. Due to that, for the next simulations we use the natural frequency.

Second comparison is for different values of K, this represent the difference between two kind of spring materials. Because of different K, we have different values of natural frequency. As we saw before the first simulation, the natural frequency depends on the mass and the stiffness.

m_{total}	10’5 g
$\frac{C_{d,c}}{C_{l,c}}$	0’1
L	0’1 m
g	9’8 $\frac{m}{s^2}$

Table 9: Common values for stiffness representations.

The values of K studied are 381,1 and 403,4 $\frac{N}{m}$ so the natural frequencies are:

K=381,1$\frac{N}{m}$	$w_n = 190'51 \frac{rad}{s}$
K=403’4 $\frac{N}{m}$	$w_n = 196'01 \frac{rad}{s}$

Table 10: Natural frequencies values for stiffness representations.

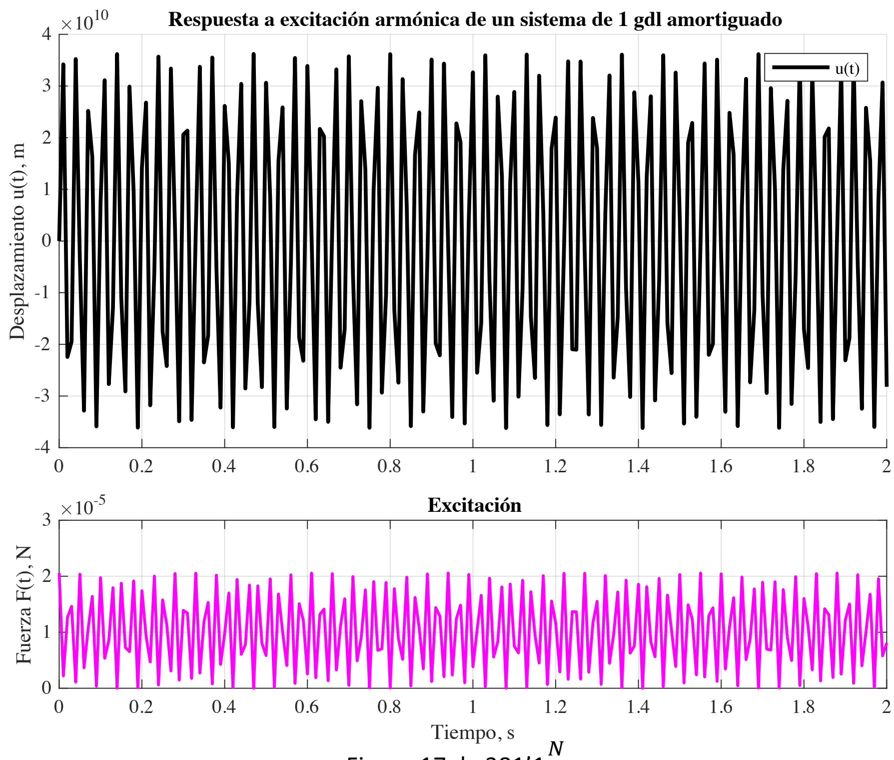

Figure 17: k=381’1$\frac{N}{m}$.

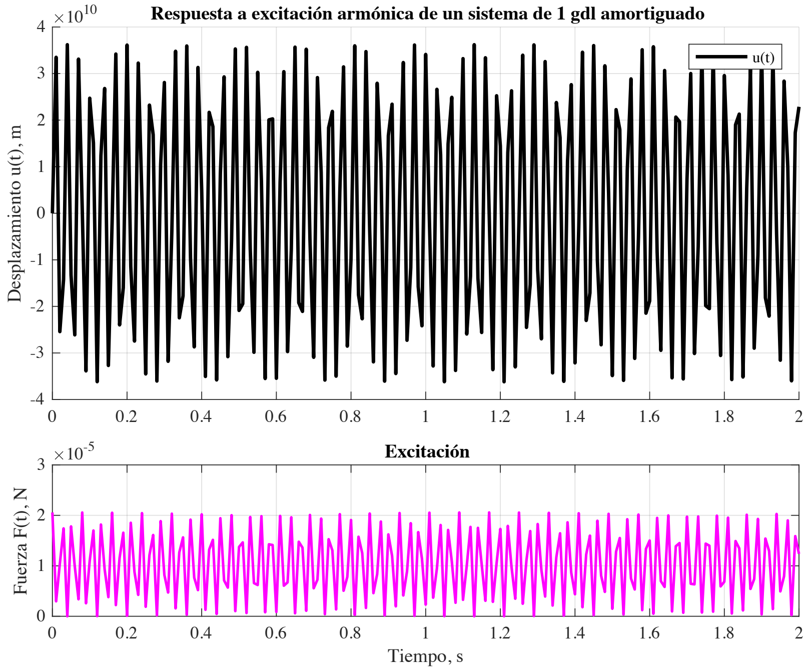

Figure 18: k=403'4 $\frac{N}{m}$.

Between this two stiffness, we can not see the difference, so both materials for the spring can be a good idea for our concepts. To see difference with the values of K, we prove values that we have not consider to our concept.

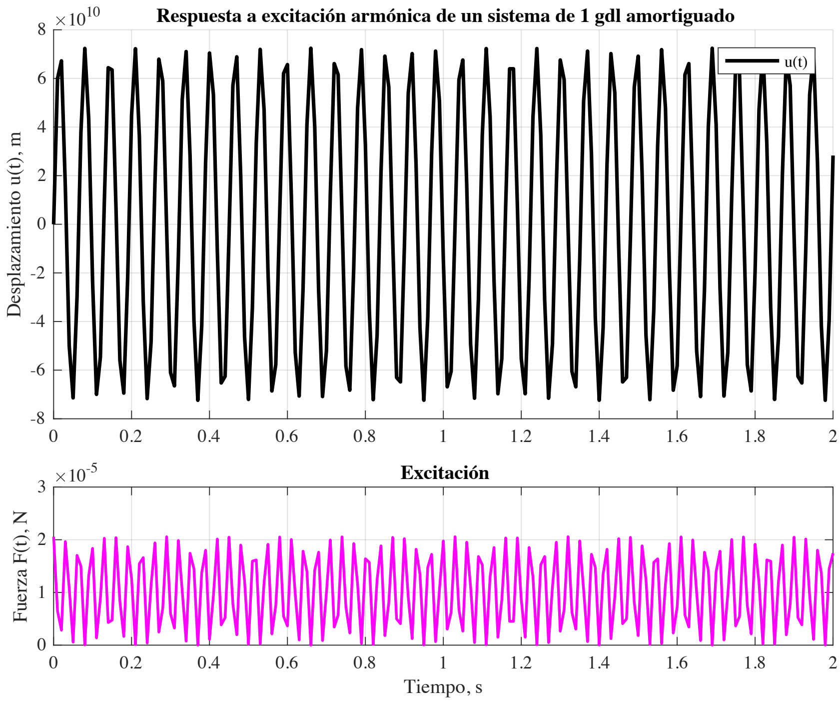

Figure 19: k=100 $\frac{N}{m}$.

As we can conclude from the figures, less stiffness produces more displacement. In spite of that, maybe we can not obtain a spring with this properties, or maybe a spring with this stiffness has less duration. More stiffness produces less movement as far as reverse movement of the system.

Third simulations are for compare the different values of the relationship between lift and drag $\frac{C_{d,c}}{C_{l,c}}$. The two values that we simulate are the borders of the range given by Ellington, $0'1 \leq \frac{C_{d,c}}{C_{l,c}} \leq 0'25$.

The rest of the values are the same as we use in the rest of simulations with the natural frequency.

$\mathbf{m_{total}}$	10’5 g
k	$381'1\ \frac{N}{m}$
$\mathbf{w_n}$	$190'51\ \frac{rad}{m}$
L	0’1 m
g	$9'8\ \frac{m}{s^2}$

Table 11: Common values for $\frac{C_{d,c}}{C_{l,c}}$ representations.

As we can see down below, the increment of the value of the relationship between lift and drag produces a growth of the value of the external force. It produces in turn an increment in the value of the displacement because the value of the amplitude has grown.

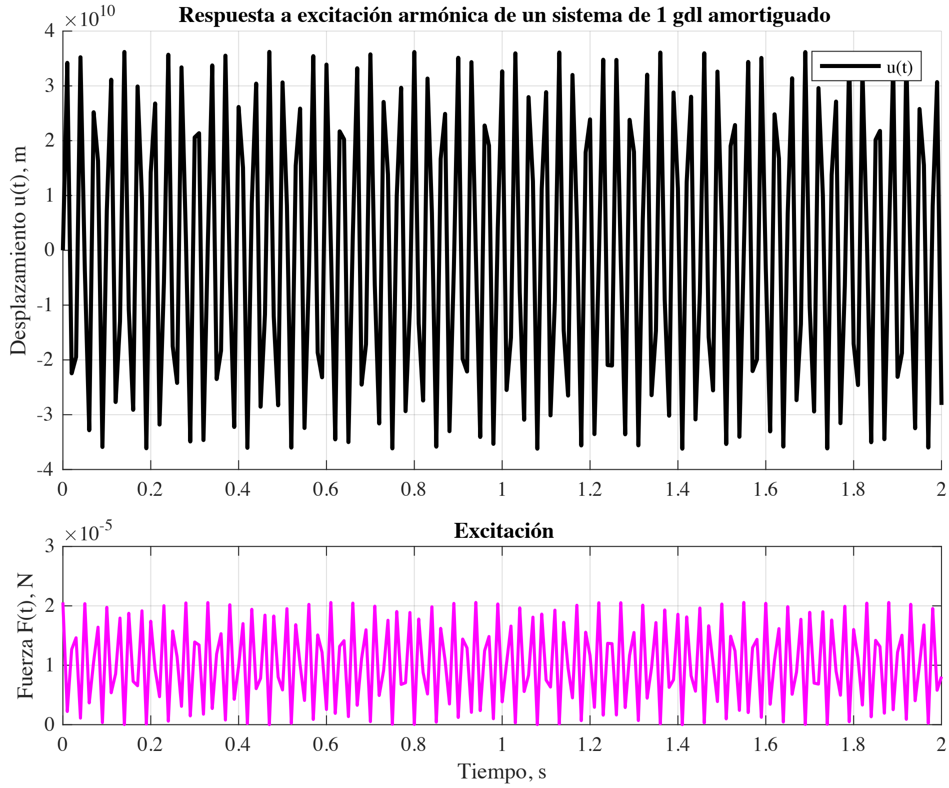

Figure 20: $\frac{C_{d,c}}{C_{l,c}}$ = 0’1.

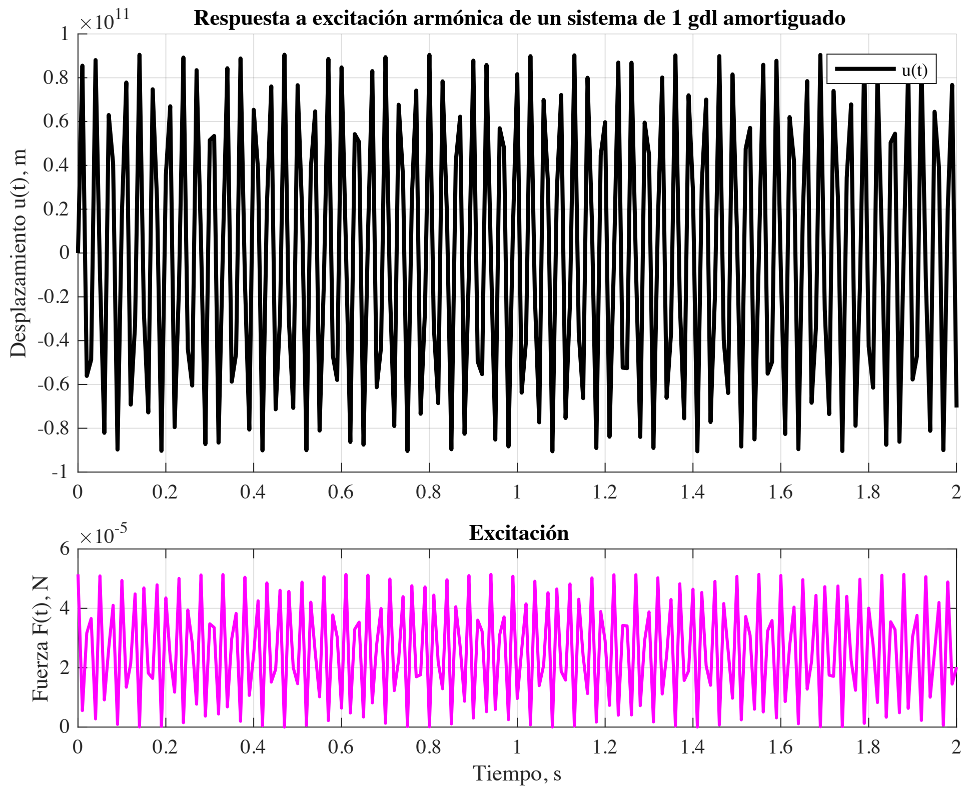

Figure 21: $\frac{C_{d,c}}{C_{l,c}}$ = 0’25.

The next comparison is for the mass case. We consider a total mass of 7 and 10’5 g. The rest of values for the simulations are the same than for the other simulations, this values are enclosed in the the following table:

$\frac{C_{d,c}}{C_{l,c}}$	0’1
k	381’1 $\frac{N}{m}$
$\mathbf{w_n}$	190’51 $\frac{rad}{m}$
L	0’1 m
g	9’8 $\frac{m}{s^2}$

Table 12: Common values for mass representations.

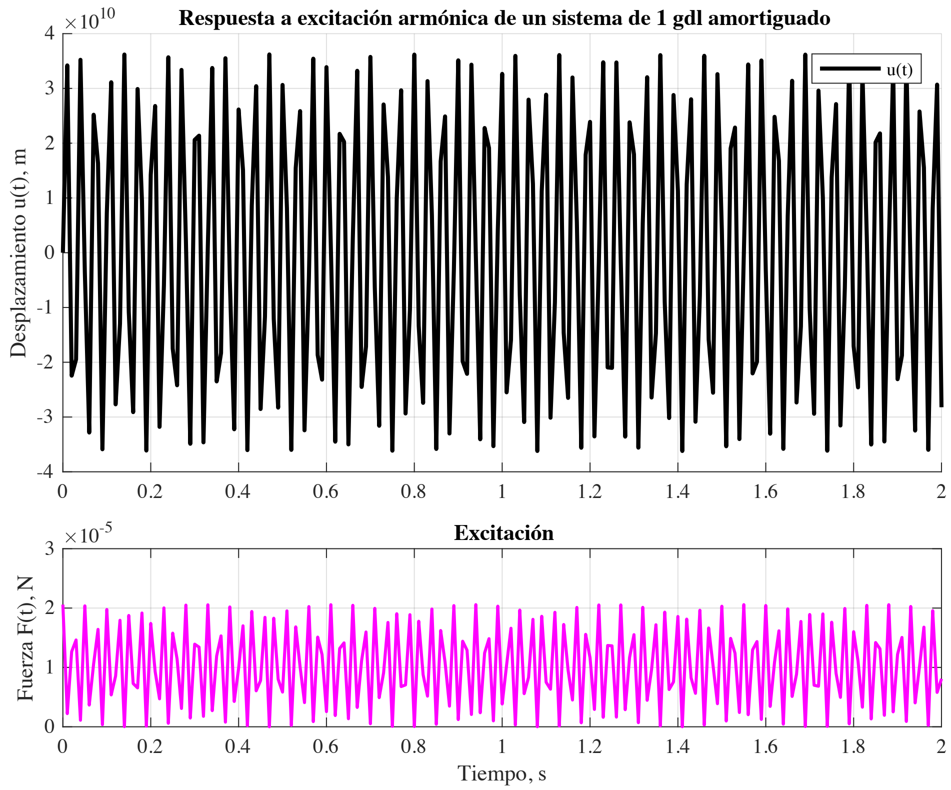

Figure 22: m_{total} = 10’5 g.

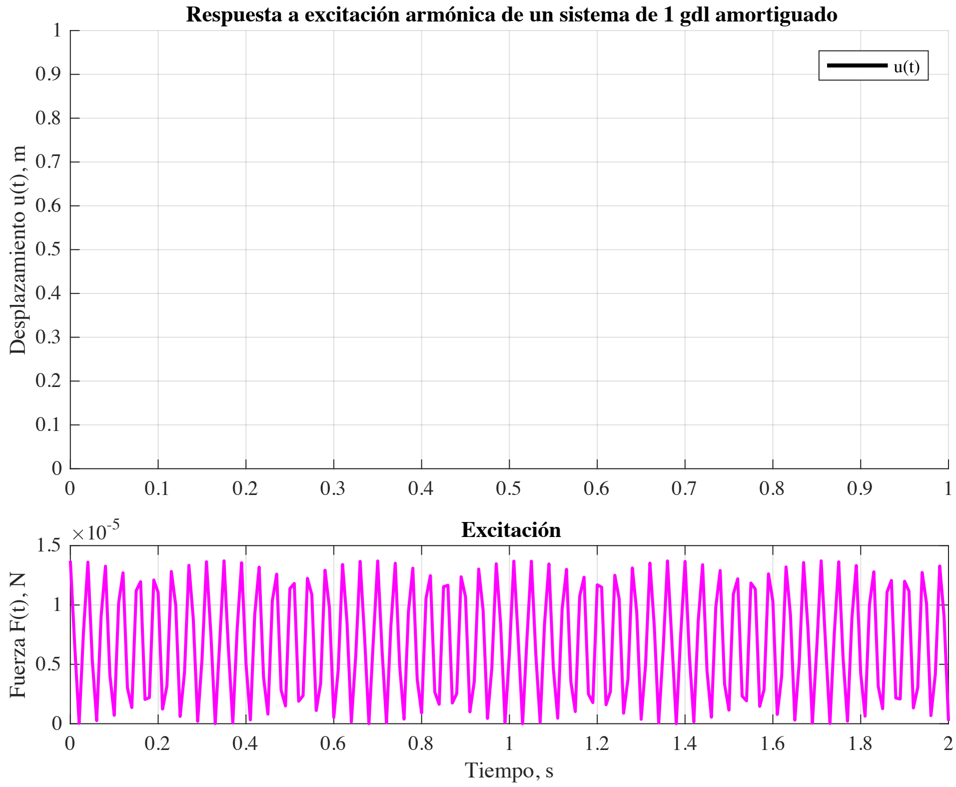

Figure 23: m_{total} = 7 g.

In conclusion, for this stiffness the concept with a mass of 7 grams has not movement. If we want a prototype lighter, with around 7 grams, we need to include a spring with less stiffness to allow the movement of the prototype and produce the flight. The Length also affects the force.

Last simulations are to compare the different length ideas for our prototypes. The two length are 10 cm and 15 cm. The rest of values are:

$\frac{C_{d,c}}{C_{l,c}}$	0’1
k	381’1 $\frac{N}{m}$
w_n	190’51 $\frac{rad}{m}$
m_{total}	10’5 g
g	9’8 $\frac{m}{s^2}$

Table 13: Common values for mass representations.

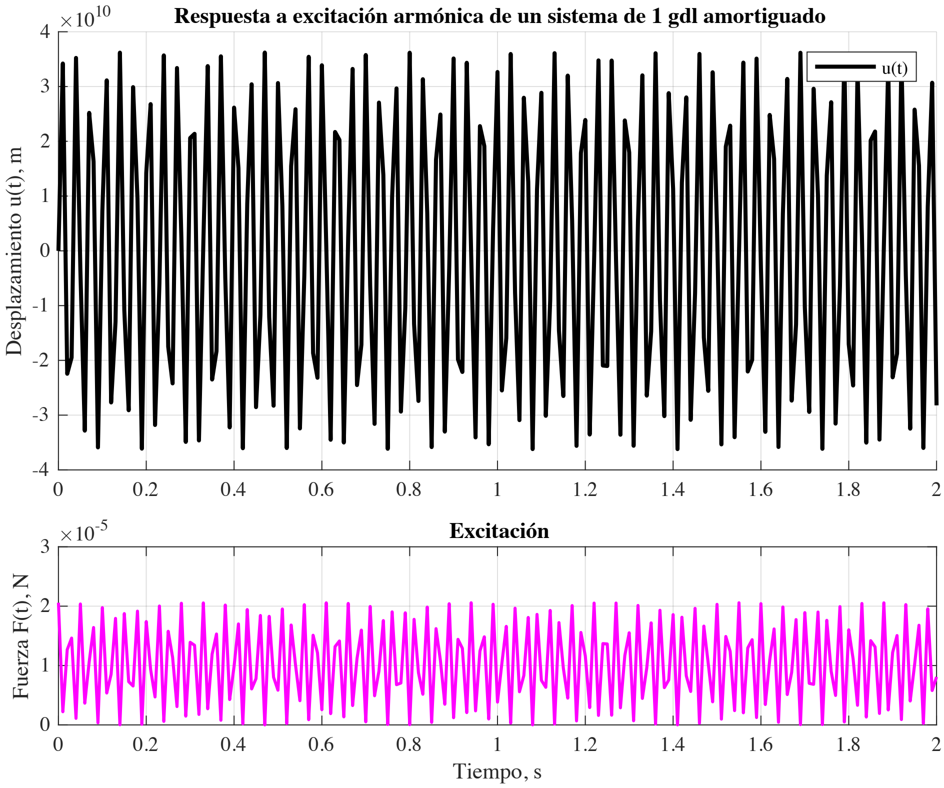

Figure 24: L = 10 cm.

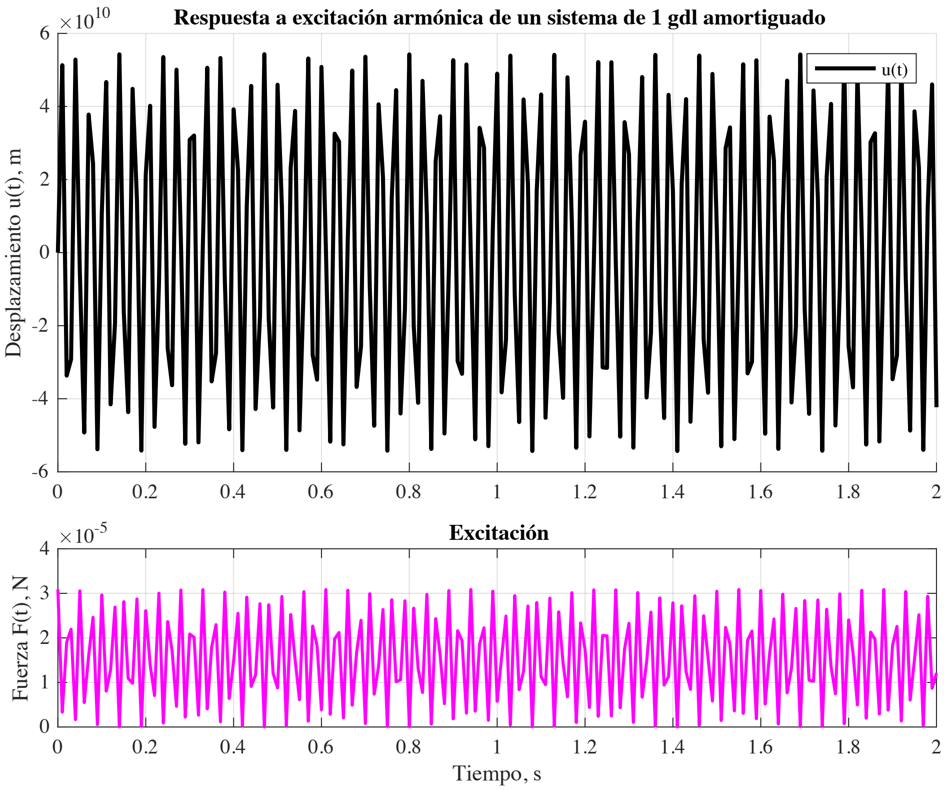

Figure 25: L = 15 cm.

As well as the rest of the variables that are present in the force, a rise of the value of the length produces a rise in the value of the displacement and of the external force.

4.5 FREQUENCY RESPONSE ANALYSIS

The frequency response is a characteristic of a system that has a measured response that is the result of a known applied input. In the case of a mechanical structure, the frequency response is the spectrum of the vibration of the structure, divided by the spectrum of the input force into the system. To measure the frequency response of a mechanical system, we must measure the spectra of the input force to the system and the vibration response. This is done more easily with a TRF analyser. Frequency response measurements are widely used in the modal analysis of mechanical systems.

The frequency response function is a three-dimensional quantity consisting of amplitude vs. phase vs frequency. That is why a true graph of it needs three dimensions, which is difficult to represent on paper. One way to do this is the Bode diagram, which consists of two curves, one of amplitude vs frequency, and one of phase vs frequency.

H(w) is the frequency response function. To calculate it, we use the following equation:

$$H(w) = \frac{1}{(k - m * w^2)} = \frac{\frac{1}{k}}{1 - r^2}$$

Where:

$$r = \frac{w}{w_n}$$

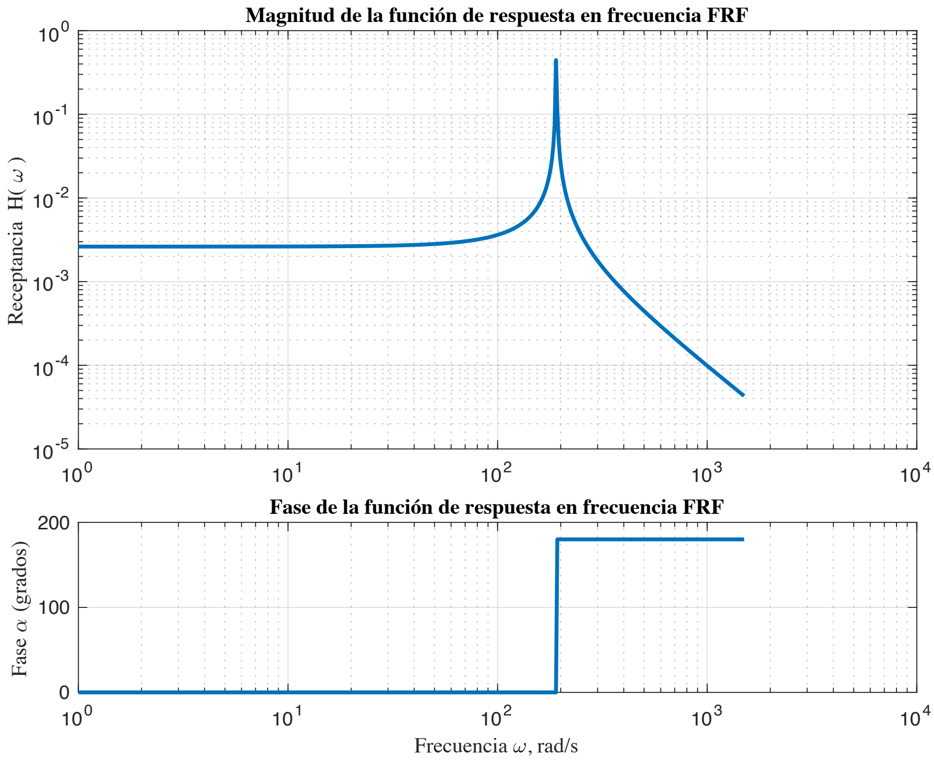

Figure 26: Frequency response function analysis.

Looking at the phase graphic, the lower plot, we can see a change of phase of 180º at the natural frequency. This is due to our system is not dumped. If our system were dumped, the change of phase would have the same magnitude but the change would be softer.

The H(w) representation shows us a maximum in the natural frequency of the system. At lower frequencies we can observe the static deflexion due to at these frequencies the stiffness has more impact.

4.6 TRANSFER FUNCTION

To check our results, we do other simulations with Matlab software. This time we use Simulink. The base of the equations to get the transfer function is the mathematical model developed in point 4.2.

$$I\ddot{\phi} + k\phi = M_{act} - M_d\dot{\phi}$$

Where:

$$I = m_{wing} * L_{total}$$

$$M_{act} = L_{wingroot} * F * \sin(w_n * t)$$

$$M_d = 2 * \frac{C_{d,c}}{C_{l,c}} * L_{wing} * m_{total} * g$$

M_{act} is a torque applied in the wing root.

Doing Laplace transform and solving the equation we get our transfer function.

$$G(s) = \frac{\phi}{u} = \frac{\phi}{F * \sin(w_n * t)} = \frac{L_{wingroot}}{s^2 * (I + M_d) + k}$$

$$G(s) = \frac{L_{wingroot}}{s^2 * \left(m_{wing} * L_{total} + 2 * \frac{C_{d,c}}{C_{l,c}} * L_{wing} * m_{total} * g\right) + k}$$

The numerical data are:

$L_{wingroot}$	1’5 cm
m_{wing}	0’096 g
L_{total}	15 cm
$\frac{C_{d,c}}{C_{l,c}}$	0’1
L_{wing}	6 cm
m_{total}	10’5 g
g	9’8 $\frac{m}{s^2}$
k	381’1 $\frac{N}{m}$

Table 14: Values for transfer function.

So our transfer function is:

$$G(s) = \frac{0'015}{s^2 * 0'0012492 + 381'1}$$

We prepare the Simulink with a sinusoidal entry and we get:

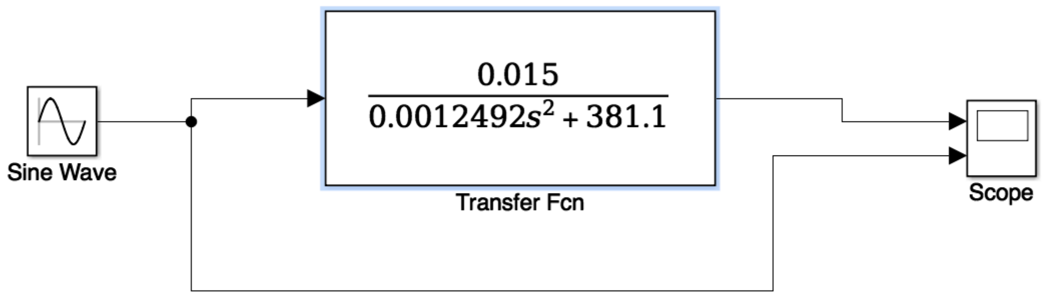

Figure 27: Simulink model.

We simulate for natural frequency and for frequency of 50 $\frac{rad}{s}$:

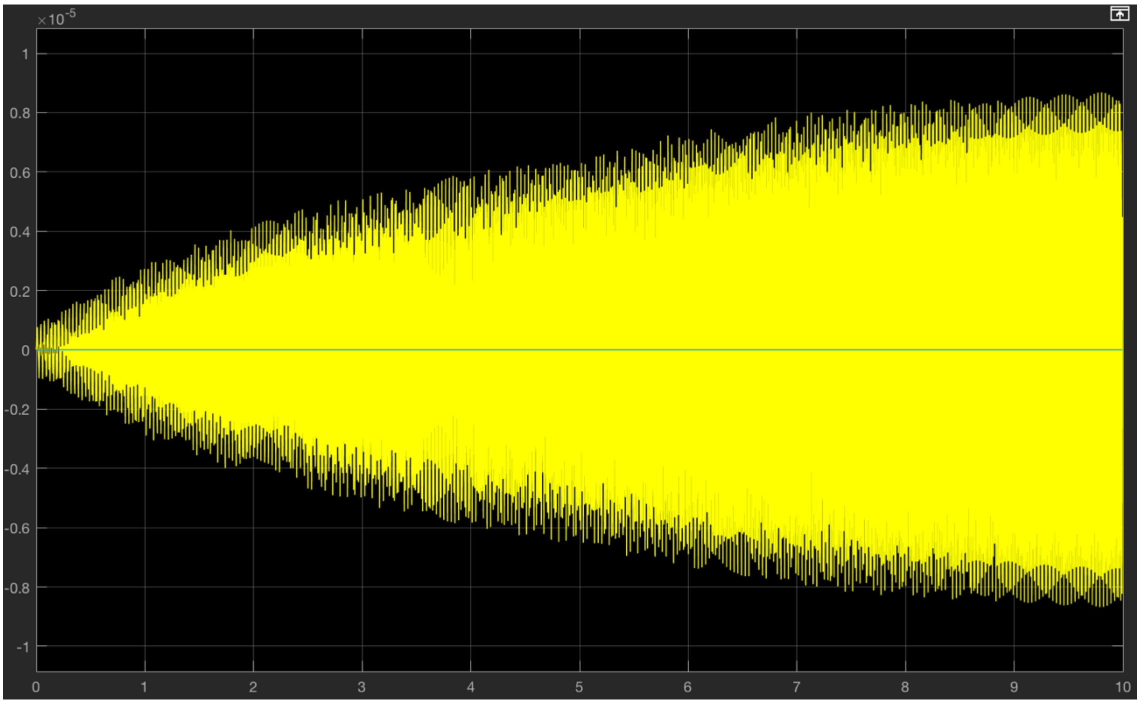

Figure 28: $G(s)$ with natural frequency input.

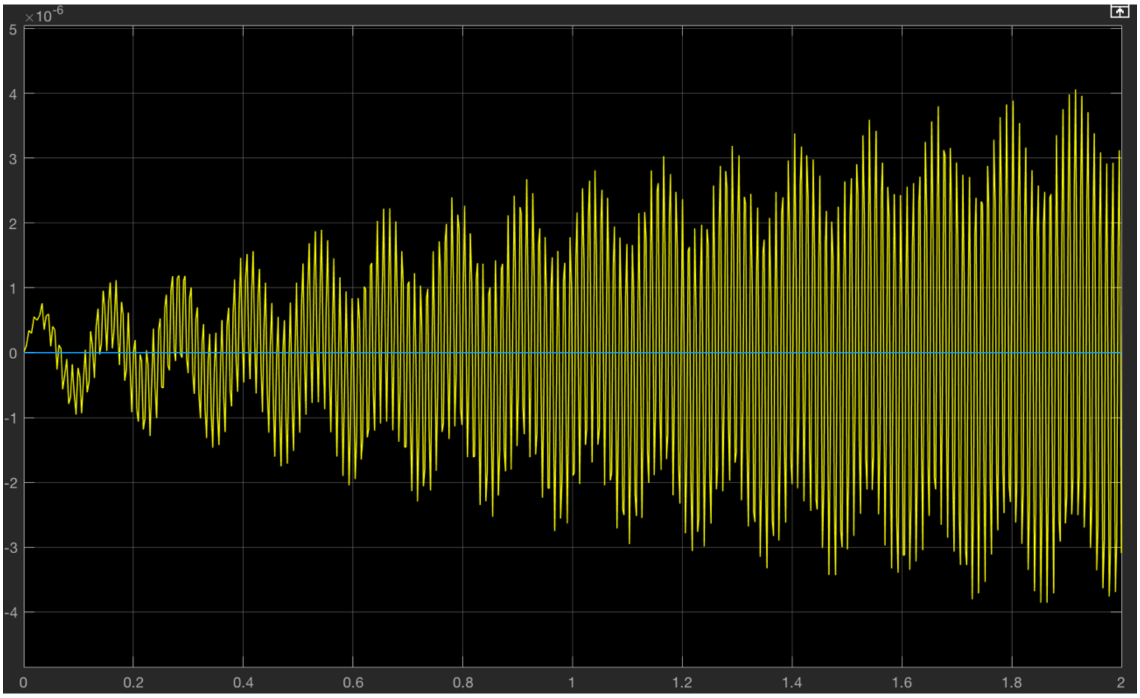

Figure 29: $G(s)$ with w=50 rad/s.

We can observe how for the natural frequency we obtain faster resonance and bigger displacements comparing with the response with w=50 $\frac{rad}{s}$. The same as with the other process.

Also, we can see the plot of the sinusoidal input:

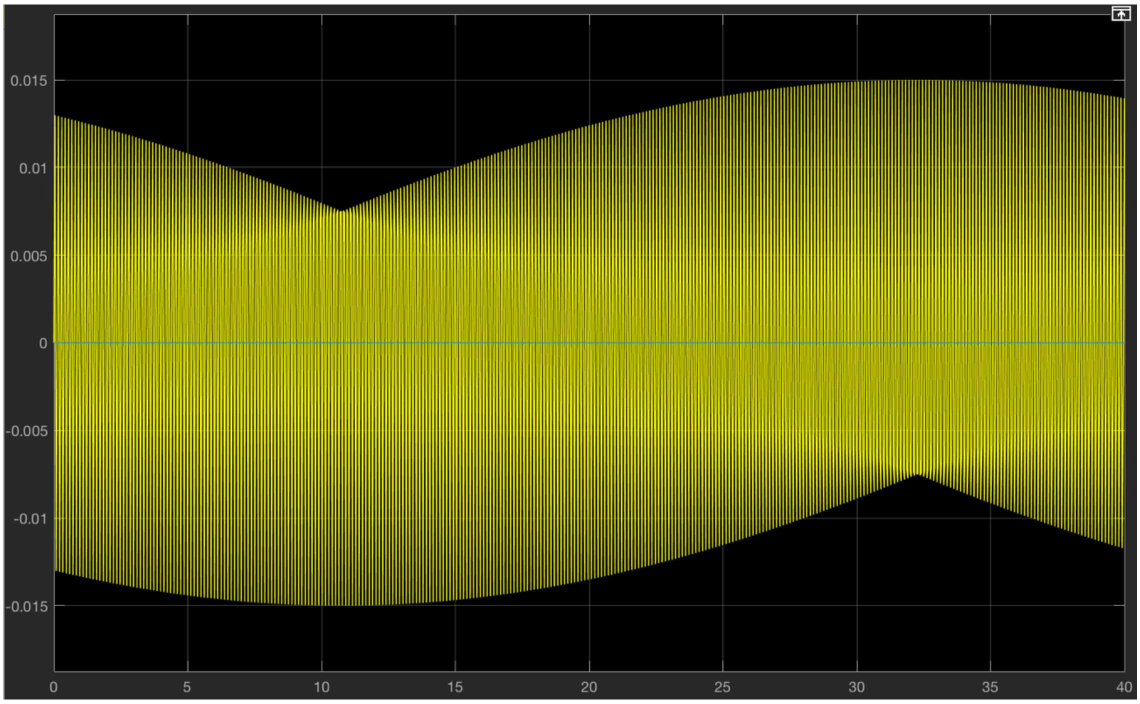

Figure 30: Input with natural frequency and amplitude of 1’5cm.

5 Conclusion

After the process of making the project. We can conclude that is possible to do a prototypes which can imitate the flight of the insects.

As we can read in firsts points, it is too difficult nowadays to produce an exact copy of the insects, but technology is developing and maybe in some years we are able to make an exact imitation to the insects.

About our idea for the prototypes. After the experimentation with Matlab, we can affirm some aspects:

- Both values for K are good. The stiffness that we have think allow sufficient displacement and movement of the prototypes and are materials that we can find in the market.
- The size of the concept needs to be the second sizing made. With the first sized concept, we obtain some problems because is too light for this stiffness.
- The lift and drag ratio interval given by Ellington can be used. If we choose the upper value, the force applied is major so the displacement is major.
- Following those guidelines, our prototype can produce the natural frequency and in that way imitate the flight of the insects.

6 Bibliography

Flapping wing actuation using resonant compliant mechanism. Author: Caspar Titus Bolsman.

Función de transferencia y respuesta en frecuencia. Escuela San Felipe.

Práctica 2: Modelizado y Simulación de Sistemas No Lineales. Escuela de Ingeniería de Cádiz.

On the quasi-steady aerodynamics of normal hovering flight part I: the induced power factor. Author: Mostafa Nabawy and William J. Crowther.

Biologically inspired hovering flight stabilization for the flapping wings micro air vehicles. Author: Paweł CHOROMAŃSKI, Krzysztof SIBILSKI.

Diseño y construcción de un robot volador bio-inspirado. Author: Sebastián Ignacio Robles Gebauer.

Aerodinámica inestacionaria y no-lineal de micro vehículos aéreos de alas batientes inspirados en la biología. Author: Bruno A. Roccia.

Design and Performance of Insect-Scale Flapping-Wing Vehicles. Author: Whitney, John Peter.

http://www.acxesspring.com/constante-de-un-resorte.html

http://www.engineeringtoolbox.com/young-modulus-d_417.html